Analytical and Bioanalytical Chemistry
https://doi.org/10.1007/s00216-018-1149-9

RESEARCH PAPER

Molecular switch-modulated fluorescent copper nanoclusters for selective and sensitive detection of histidine and cysteine

Zefeng Gu[1] · Zhijuan Cao[1]

Received: 13 March 2018 / Revised: 26 April 2018 / Accepted: 16 May 2018

Abstract

A novel assay for histidine and cysteine has been constructed based on modulation of fluorescent copper nanoclusters (CuNCs) by molecular switches. In our previous work, a dumbbell DNA template with a poly-T (thymine) loop has been developed as an excellent template for the formation of strongly fluorescent CuNCs. Herein, for the first time, we established this biosensor for sensing two amino acids by using dumbbell DNA-templated CuNCs as the single probe. Among 20 natural amino acids, only histidine and cysteine can selectively quench fluorescence emission of CuNCs, because of the specific interaction of these compounds with copper ions. Furthermore, by using nickel ions (Ni^{2+}) and N-ethylmaleimide as the masking agents for histidine and cysteine respectively, an integrated logic gate system was designed by coupling with the fluorescent CuNCs and demonstrated selective and sensitive detection of cysteine and histidine. Under optimal conditions, cysteine can be detected in the concentration ranges of 0.01–10.0 μM with the detection limit (DL) of as low as 98 pM, while histidine can be detected in the ranges of 0.05–40.0 μM with DL of 1.6 nM. In addition, histidine and cysteine can be observed with the naked eye under a hand-held UV lamp (DL, 50 nM), which can be easily adapted to automated high-throughput screening. Finally, the strategy has been successfully utilized for biological fluids. The proposed system can be conducted in homogeneous solution, eliminating the need for organic cosolvents, separation processes of nanomaterials, or any chemical modifications. Overall, the assay provides an alternative method for simultaneous detection of cysteine and histidine by taking the advantages of high speed, no label and enzyme requirement, and good sensitivity and specificity, and will satisfy the great demand for determination of amino acids in fields such as food processing, biochemistry, pharmaceuticals, and clinical analysis.

Keywords Dumbbell DNA template · Histidine · Cysteine · Logic gate · Fluorescent copper nanoclusters

Introduction

Amino acids are the basic components of various biomacromolecules which are vital to life and have many functions in cellular metabolism. Because of its specific side group, each amino acid plays unique functions in biological processes [1]. Among the 20 natural amino acids, both histidine (His) and cysteine (Cys) have attracted attention in recent years due to their critical bioactivities and functions, as well as their involvement in certain diseases. For example, Cys deficiency is associated with many syndromes, such as slow growth of children, hair depigmentation, edema, lethargy, liver damage, loss of muscle and fat, skin lesions, and weakness [2, 3]. On the other hand, an elevated Cys level was reported to induce hypoglycemic brain damage and neurotoxicity, an alternative mechanism to excitotoxicity [4]. Similarly, His plays an essential role in the growth and repair of tissues. It controls the transmission of metallic elements in biological bases, preserves the integrity of myelin sheaths, and protects the body from damage caused by radiation [5]. Furthermore, as a precursor amino acid of histamine, histidine is involved in inflammatory response, cellular growth and differentiation, regulation of nucleic acids, and protein synthesis. Abnormal levels of histidine may cause psychological disorders, rheumatoid arthritis, nerve deafness, and many other diseases [5–7].

Many efforts have been directed to the development of detection methods for Cys and His, including flow injection

Electronic supplementary material The online version of this article (https://doi.org/10.1007/s00216-018-1149-9) contains supplementary material, which is available to authorized users.

✉ Zhijuan Cao
zjcao@fudan.edu.cn

[1] School of Pharmacy, Fudan University, 826 Zhangheng Road, Shanghai 201203, China

Published online: 07 June 2018

analysis [8, 9], microfluidic analysis [10], liquid chromatography [11, 12], electrochemical detection and electrochemiluminescent analysis [13, 14], resonance light scattering [15], and photochemical vapor generation atomic spectrometry [16]. Recently, fluorimetric and colorimetric sensors have been extensively used for amino acid detection with the advantages of convenience, sensitivity, and selectivity [17–27]. These amino acid chemosensors have been designed via several strategies such as competitive displacement assays, metal-ligand interaction, metal-ligand exchange, and specific reactions between chemosensors and amino acids. For example, Shao et al. reported that thiol-containing amino acids can interact with metal ion-binding spiropyran, resulting in appreciable changes in color and absorption properties of spiropyran [18]. Sun et al. reported an indicator-displacement assay for visual detection of histidine with murexide as the indicator [19]. The competition of histidine and murexide for binding with Ni^{2+} resulted in a color change from yellow to purple. However, when it comes to probes designed for the simultaneous detection of two amino acids, there have been only a few reports [28–32]. Pu et al. developed a fluorescence assay for detection of cysteine and histidine. Fluorescent thiazole orange (TO) shows intense fluorescence upon interaction with a DNA probe, and divalent metal ions act as quenchers [28]. A G-quadruplex was used to establish a fluorescence sensor for the detections of His and Cys by using N-methylmesoporphyrin IX or G-quadruplex-copper (II) metalloenzyme as the reporter [29, 31]. Overall, there is of great practical need to develop more simple and sensitive simultaneous biosensors for two or more amino acids with one probe in a facile format.

Fluorescent metal nanoclusters (NCs), including gold, silver, platinum, and copper NCs, have been developed to be a new type of nanomaterial with fascinating properties such as low toxicity, remarkable water solubility, facile synthesis, large Stokes shifts, and good biocompatibility [33, 34]. In particular, DNA-scaffolded fluorescent nanomaterials have shown robust and promising applications in fluorescent biosensing and imaging [35]. DNA-templated fluorescent copper nanoclusters (CuNCs) have been employed for sensing various targets because double-strand DNA and linear poly-T single-strand DNA can be utilized as efficient templates to form fluorescent CuNCs based on the interaction between copper ions and nucleobases, especially thymine [36, 37]. In previous work, our group reported that a dumbbell DNA with poly-T loop could be a promising template for the formation of CuNCs [38]. The DNA structure was composed of a poly-T loop region and a random dsDNA stem. By comparison of previous templates, these new dumbbell DNA-templated CuNCs exhibited improved fluorescent properties for biochemical sensing.

Herein, we report a simple and sensitive CuNC-based strategy for the simultaneous detection of histidine and cysteine based on four molecular switches, including His, Cys, Ni^{2+}, and N-ethylmaleimide (NEM). In this approach, first, the strongly fluorescent CuNCs are formed by dumbbell DNA-templated CuNCs, which signal is quenched by His or Cys because these two amino acids can competitively bind copper ions from a DNA sequence and induce CuNC aggregation. After that, Ni^{2+}/NEM can correspondingly snatch His/Cys to recover the fluorescent emission [19]. Based on that, His and Cys could be selectively determined by using a single-probe CuNC. Finally, the sensing system was tested in a biological fluid.

Experimental

Chemicals and materials

All oligonucleotides used in this work were synthesized by KareBayTM Biochem, Inc. (Ningbo, China) and purified by HPLC. The sequences of the DNA oligonucleotides are listed in Table 1.

Cysteine (Cys), histidine (His), glycine (Gly), alanine (Ala), valine (Val), leucine (Leu), isoleucine (Ile), proline (Pro), phenylalanine (Phe), tyrosine (Tyr), tryptophan (Trp), serine (Ser), threnonine (Thr), methionine (Met), asparagine (Asn), aspartic acid (Asp), glutamic acid (Glu), lysine (Lys), arginine (Arg), ornithine (Orn), and taurine (Tau) were all purchased from Sigma Aldrich (St. Louis, MO). Nickel chloride ($NiCl_2$), 3-(N-morpholino)-propane sulfonic acid (MOP), ascorbic acid, and copper sulfate pentahydrate ($CuSO_4 \cdot 5H_2O$) were obtained from Sinopharm Chemical Reagent Co., Ltd.

Table 1 DNA sequences used in the work

Name	Sequences (5′-3′)
Loop1	TGATGACCA T_{30} TGGTCA TCAGAA CTTCAG T_{30} CTGAA GTTC
Loop2	TGATGA CCA T_{20} TGGTCA TCAGAA CTTCAG T_{20} CTGAA GTTC
Loop3	GTTCT T_{30} AGA ACA G T_{30} CTG AA
Loop4	GCG TGA TGA CCA T_{10} TGG TCA TCA CGC GCG GAA CTT CAG T_{10} CTG AAG TTC CGC
Sequence 5	T_{40}
Sequence 6	T_{30}

(Shanghai China). N-Ethylmaleimide (NEM) was purchased from Shanghai Reminder Co. Ltd. (Shanghai, China). All chemicals were of analytical grade. All stock and buffer solutions were prepared in distilled water purified by a Milli-Q water purification system (Millipore Corp., Bedford, MA) with an electrical resistance of 18.2 MΩ at 25 °C. MOP buffer solution (10 mM MOPs, 250 mM NaCl, pH = 7.5) was used as the reaction buffer and CuNC preparation buffer in this study.

Apparatus

All fluorescence measurements, including emission spectra and fluorescence intensity, were performed on an F-7000 spectrofluorometer (Hitachi, Japan). Both the excitation and emission bandpasses were set at 10 nm. Fluorescence emission spectra were collected from 550 to 670 nm with a 355-nm excitation wavelength. The fluorescence spectra were measured in a 1-mL quartz cuvette. All fluorescence measurements were performed at room temperature (25 °C). Fluorescence emission photographs of CuNCs were obtained by Canon 50D cameras under UV irradiation. Particle sizes of CuNCs in the absence and presence of amino acid were characterized by a Nano-ZS (Malvern, UK). Transmission electron microscopy (TEM) images were obtained using a FEI Tecnai G2S-TWIN electron microscope (FEI, MD, USA).

Preparation of CuNCs and detection procedure

In a typical procedure, first, stock solutions of template DNA were diluted to desired concentration with MOP buffer. Then, $CuSO_4$ was added to the DNA solutions and mixed completely. Finally, ascorbic acid was added and incubated for 20 min at room temperature (25 °C) to form fluorescent CuNCs.

To detect histidine, various concentrations of His solution (mixed with a certain concentration of Cys) in 100 μL MOP buffer were placed in a 1.7-mL calibrated test tube. Then, 10 μL NEM (2 mM), 5 μL $CuSO_4$ solution (2 mM), and 50 μL of template DNA were sequentially added to mix with His solution. MOP buffer was added to dilute the mixture to a volume of 0.2 mL. After mixing completely, ascorbic acid was added as the reducing reagent. The mixture was vortexed to mix all the reagents dramatically and then incubated for 20 min at room temperature to form the fluorescent CuNCs. To detect cysteine, a different concentration of Cys solution (100 μL with a certain concentration of His), 10 μL $NiCl_2$ (2 mM), 5 μL $CuSO_4$ (2 mM), and 50 μL of template DNA were mixed and diluted to 0.2 mL with MOP buffer. Ten microliters of ascorbic acid was added, and the mixed solution was kept for 20 min at room temperature, followed by measurement of the fluorescence emission spectrum or image capture under UV irradiation.

Detection of His and Cys in urine samples

Urine samples were collected from healthy volunteers and used after filtering by membrane (0.22 μm, Truelab, Shanghai, China) and dilution with MOP buffer. Spiked samples were prepared by introducing His/Cys into the diluted urine samples. To determine histidine in diluted urine samples, the spiked diluted samples (100 μL) and 10 μL NEM (2 mM) were mixed first. For Cys detection, 10 μL Ni^{2+} (2 mM) was added to the spiked urine samples. Subsequently, 5 μL $CuSO_4$ solutions and 50 μL of template DNA were sequentially added to a test tube. The reaction solution was diluted with MOP buffer to a volume of 0.2 mL. The mixture was vortexed and equilibrated for 1 min. Ten microliters of ascorbic acid was then added, and the resulting solution was shaken thoroughly and equilibrated for 20 min at room temperature before fluorescence emission spectra measurement.

Results and discussion

Design of molecular switch-modulated CuNC biosensor for His and Cys

The principles of the amino acid biosensor based on fluorescent CuNCs are depicted in Fig. 1. The DNA template consists of a 30-thymine loop and 10-mer random ds DNA stem with a nick point. For the synthesis of DNA-templated CuNCs, the DNA template binds to copper ions and provides the necessary microenvironment for the reduction of copper ions. Strongly fluorescent CuNCs form when the copper ions are reduced by ascorbic acid. Upon addition of His or Cys, the fluorescence signal is obviously quenched. As demonstrated in previous works [29, 31], NEM is a common Cys scavenger and Ni^{2+} is a recognized His-binding metal ion. Thus, Ni^{2+} and NEM were employed for the selective detection of Cys and His, respectively. The fluorescence intensity is related to the concentrations of added His/Cys. When the two masking reagents are added together to the sensing solution, strong fluorescence can be restored.

Evaluation of the quenching activity of His/Cys on the fluorescence signal of CuNCs

In this design, His and Cys were reported to have higher coordination reactivity with copper ions compared to sole carboxyl group [39, 40]. Therefore, it is understandable that the addition of amino acid (His/Cys) will quench the fluorescence emission, which has been further confirmed from fluorescence spectra, TEM images, and particle size data. As shown in Fig. 1, we initially observe the obvious decrease of fluorescence emission intensity with the addition of His/Cys. As demonstrated by TEM images in Fig. 2, the introduction of His or

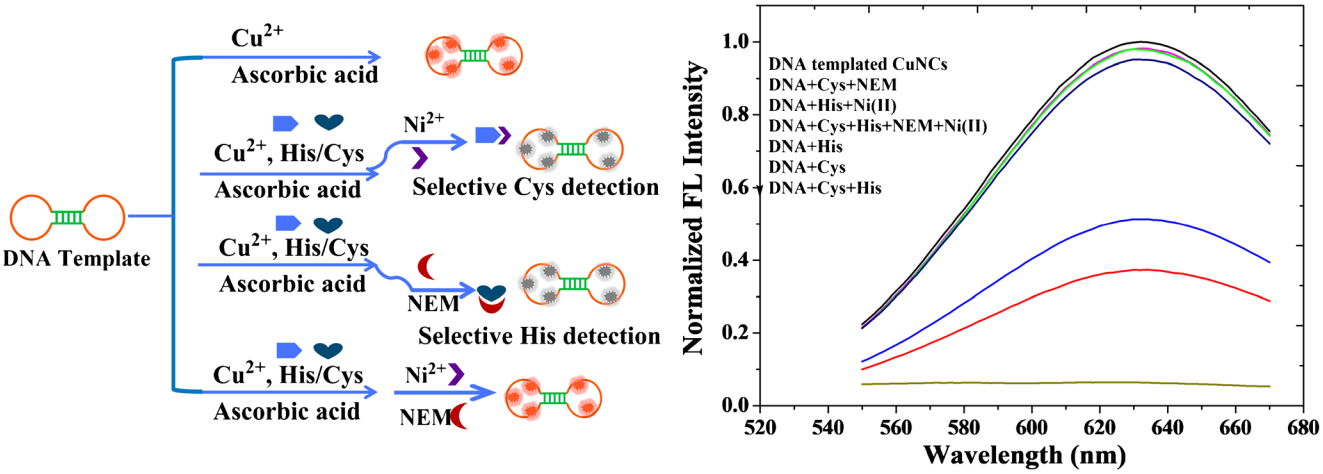

Fig. 1 Schematic principle of molecular switch-modulated CuNCs for the detection of amino acids. Measurements were performed by using 0.375 μM Loop 3, 50 μM $CuSO_4$, 0.75 mM ascorbic acid, 12.5 μM amino acids, and 100 μM Ni^{2+}/NEM in MOP buffer. From the top to the bottom, the black, magenta, green, navy, blue, red, and dark yellow lines correspond to the FL signal of CuNCs generated by DNA template, DNA+Cys+NEM, DNA+His+Ni(II), DNA+Cys+His+NEM+Ni(II), DNA+His, DNA+Cys, and DNA+Cys+His

Cys induces obvious aggregation of the CuNCs. In Fig. S1 in the Electronic Supplementary Material (ESM), the average size of Loop 3-templated CuNCs is calculated to be about 2.6 nm. However, in the presence of His and Cys, the particle sizes of CuNCs are enhanced to be 615 and 859 nm, respectively. A larger DLS particle size than that measured by TEM was obtained due to hydrophilization (please see more detail in the ESM). Thus, the fluorescence quenching of CuNCs is due not only to the competitive binding of amino acids to copper ions from the template DNA but also to the binding-induced aggregation of CuNCs.

Optimization of experimental parameters and selective detection of His/Cys

DNA-scaffolded CuNCs were synthesized by reducing copper ions with ascorbic acid in the presence of different types of DNA templates, including linear poly-T with different lengths, and dumbbell DNA with different loop and stem lengths. The fluorescence emission spectrum of each sample of DNA-templated CuNCs with the same concentration is recorded in Fig. S2a (see ESM). First, each DNA template shows different ability to form the fluorescence CuNCs in the order of Loop 3 (T_{30}-loop, 10-bp stem) > Loop 1 (T_{30}-loop, 18-bp stem) > T_{40} > Loop 2 (T_{20}-loop, 18-bp stem) > T_{30} > Loop 4 (T_{10}-loop, 24-bp stem). All the as-prepared CuNCs exhibit fluorescence emission in the range of 600–635 nm with excitation at 355 nm. Among the designed DNA templates, Loop 3 template was demonstrated to be optimal for the formation of fluorescent CuNCs. As shown in Fig. S2b (see ESM), we get the best fluorescent ratio $[(I_0\text{-}I)/I_0]$ for Cys detection with Loop 4 as the template, but not for His. However, the fluorescent intensity of Loop 4 is relatively low. Overall, Loop 3-templated CuNCs are the most sensitive for the detection of two amino acids in the order of Loop 3 > Loop 2 > Loop 1 > Loop 4 > $T_{40} = T_{30}$ (see ESM Fig. S2b). Therefore, dumbbell DNA templates are

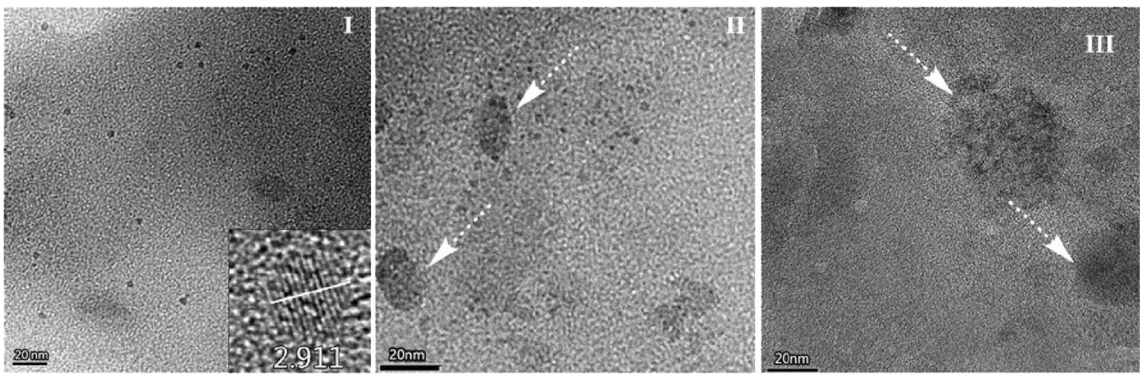

Fig. 2 TEM images of Loop 3-templated CuNCs in the absence (I) and presence of His (II) or Cys (III). Measurements were performed using 0.25 μM Loop 3, 50 μM $CuSO_4$, 0.75 mM ascorbic acid, and 12.5 μM amino acids in MOP buffer. After formation, the CuNCs were fivefold diluted with pure water before measurement

helpful to get better sensitivity. Finally, Loop 3 template was used in the subsequent experiments.

Selection of other parameters

Since many other factors will affect the fluorescent CuNC-based sensing system of amino acids, the influences of these factors were studied respectively, including the amounts of DNA template, copper ions, and ascorbic acid. First, the concentration of ascorbic acid was an important factor for fluorescent intensity of CuNCs. As shown in Fig. S3A, a, (see ESM), the ratio of the fluorescent signal before and after the addition of His/Cys $[(I_0\text{-}I)/I_0]$ reached the optimal one with 0.75 mM ascorbic acid from 0.5 to 1.75 mM. Second, considering the binding and aggregation ability of His/Cys on the CuNC system, the concentration of copper ions (Cu^{2+}) significantly affects the sensing of His/Cys. Fluorescent intensity ratio $[(I_0\text{-}I)/I_0]$ increased with the increasing of Cu^{2+} concentration from 12.5 to 50 μM and then decreased, which indicated that 50 μM Cu^{2+} maximally favored the sensing of His/Cys (see ESM Fig. S3B, b). Lower Cu^{2+} concentration is not suitable for the formation of strongly fluorescent CuNCs. If Cu^{2+} is superfluous, however, more amino acids would be required to snatch Cu^{2+} from DNA template, which is not benefit to reach a low detection limit. Third, as shown in Fig. S3C, c (see ESM), higher concentration of the template is helpful to get a better fluorescent intensity and intensity ratio $[(I_0\text{-}I)/I_0]$ of sensing His/Cys in the range of 0.0625–0.375 μM. However, too many DNA templates will need more Cu^{2+} for the formation of fluorescent CuNCs, and then not benefit for the sensitive detection of His/Cys. Overall, the concentration of ascorbic acid, copper ions, and DNA template was set at 0.75 mM, 50 μM, and 0.375 μM respectively in the following study.

Selectivity of the sensing system against other amino acids

To test the selectivity for His and Cys, 21 essential amino acids were treated individually with the molecular switch-tuned fluorescent CuNC system. The fluorescence intensity for each amino acid was recorded and compared with the control fluorescence signal in the absence of amino acids. As shown in Fig. 3, both His and Cys could seize copper ions from the copper ion-nucleobase interaction and then induced the aggregation of CuNCs, resulting in fluorescence quenching. In comparison, other amino acids did not result in the obvious change of the fluorescence signal. The tolerance experiment of other amino acids was investigated in further. As shown in Fig. S4 (see ESM), even 40 μM of Asn, Met, and Trp, and 50 μM other amino acids could not influence the detection of His and Cys. However, when the concentration was up to 60 μM, all amino acids will quench CuNC fluorescence to influence the detection of His/Cys (more details in the ESM).

Demonstration of the integrated logic system for selective determination of His and Cys

To establish the selective sensing method, it is important to prove the corresponding masking effects of Ni^{2+} and NEM on His and Cys. We designed the CuNC-based integrated logic system as shown in Fig. 4. The fluorescent signal can be quenched by His and Cys and then recovered by Ni^{2+} and NEM, respectively. Thus, these four species can tune the fluorescent emission of CuNCs, which can be described and manipulated as molecular logic gates. His, Ni^{2+}, Cys, and NEM are used as four inputs, and 16 input modes in the truth table are employed to modulate the optical output (fluorescence

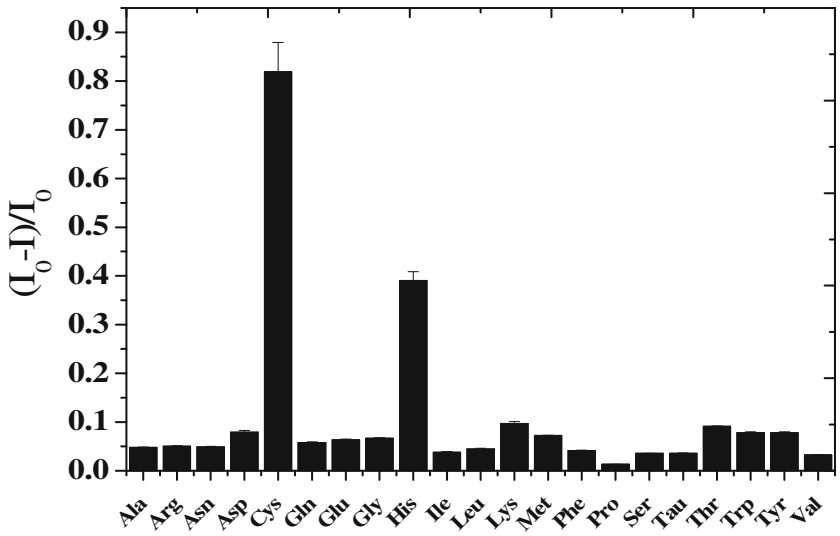

Fig. 3 Fluorescent intensity ratio $[(I_0\text{-}I)/I_0]$ for dumbbell DNA-templated CuNCs measured in the absence and presence of various individual amino acids. Measurements were performed by using 0.5 μM Loop 3, 50 μM $CuSO_4$, 0.75 mM ascorbic acid, and 12.5 μM amino acids in MOP buffer. The error bars demonstrate the standard deviation for three independent measurements

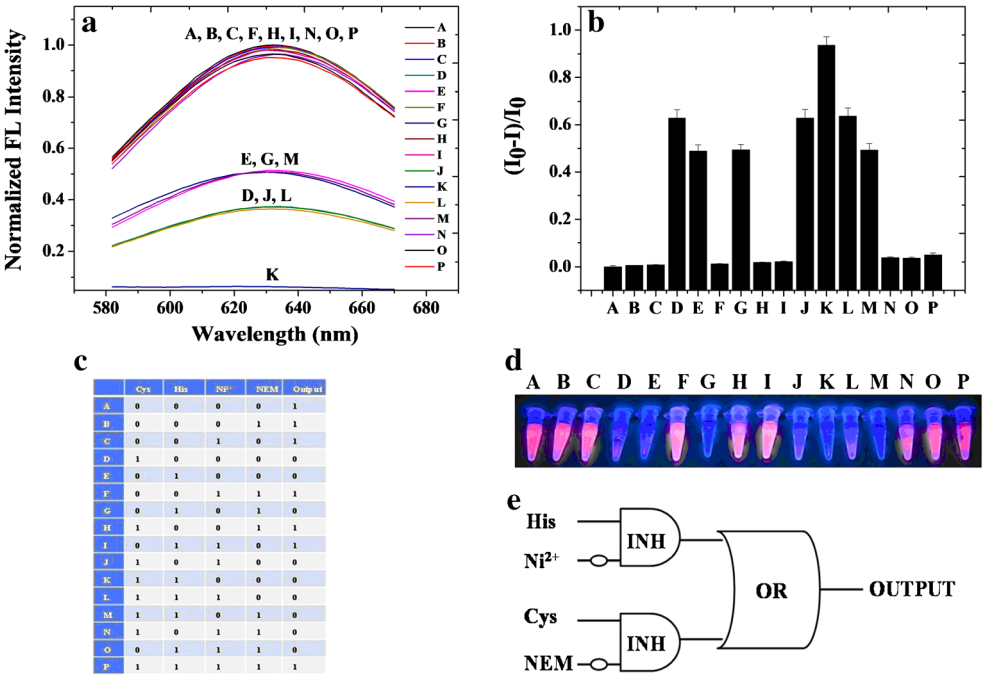

	Cys	His	Ni^{2+}	NEM	Output
A	0	0	0	0	1
B	0	0	0	1	1
C	0	0	1	0	1
D	1	0	0	0	0
E	0	1	0	0	0
F	0	0	1	1	1
G	0	1	0	1	0
H	1	0	0	1	1
I	0	1	1	0	1
J	1	0	1	0	0
K	1	1	0	0	0
L	1	1	1	0	0
M	1	1	0	1	0
N	1	0	1	1	0
O	0	1	1	1	0
P	1	1	1	1	1

Fig. 4 **a** Photograph of dumbbell DNA-templated CuNCs before or after 16 input modes. **b** FL intensity ratio $(I_0\text{-}I)/I_0$ at 630 nm for the 16 input modes, where I and I_0 are the corresponding FL intensities in the presence and absence of His/Cys. **c** Truth table for 16 input and output modes. **d** UV image for 16 input modes. **e** Logic scheme of the integrated logic system of INH (inhibition) and OR gate. Measurements were performed by using 0.375 μM Loop 3, 50 μM $CuSO_4$, 0.75 mM ascorbic acid, 12.5 μM amino acids, and 100 μM Ni^{2+}/NEM in MOP buffer

emission) (Fig. 4b). We defined the presence of His, Ni^{2+}, Cys, and NEM inputs as "1," and absence as "0." The fluorescence intensity ratio $[(I_0\text{-}I)/I_0]$ denotes the quenching efficiency of amino acids. Thus, the fluorescence intensity ratio $(I_0\text{-}I)/I_0$ (more than 0.2) was defined as the output "1," and no obvious change (with intensity ratio less than 0.2) was set as "0." As shown in Fig. 4a, in the case of no input, we observed high fluorescence intensity of DNA-templated CuNCs (**A**). To determine if the masking reagents would affect the fluorescence intensity, the following three input modes were studied, including NEM (**B**), Ni^{2+} (**C**), Ni^{2+}, and NEM (**F**). There was no obvious fluorescence decrease, demonstrating that Ni^{2+} and NEM do not influence the formation of CuNCs. And then, with the addition of either Cys or His as the input (**D**, **E**), the fluorescent intensity obviously decreased due to the amino acids seizing of Cu^{2+} from DNA template and the induced aggregation. After that, we added shielding agent (Ni^{2+} and NEM) to the reaction solution separately. That is, the following five input modes, Cys and NEM (**H**); His and Ni^{2+} (**I**); Cys, NEM, and Ni^{2+} (**N**); His, Ni^{2+}, and NEM (**O**); and Cys, NEM, His, and Ni^{2+} (**P**), were designed to elucidate inhibition ability of masking reagents on the corresponding amino acid. The fluorescence signal of CuNCs was found to be recovered to the level of **A**, corresponding to the two "INH" (inhibition) gates (Fig. 4e). However, if the masking reagent is not the correct one, can the fluorescence signal be recovered or not? With the input mode of Cys and Ni^{2+} (**J**) and Cys, His, and Ni^{2+} (**L**), it was found that the fluorescence intensity was also reduced to the same ratio as **D** (output **1**). Similarly, the fluorescence response for the input modes of His and NEM (**G**) and His, Cys, and NEM (**M**) was obtained as the same ratio as **E**. Thus, it was shown that Ni^{2+} and NEM can selectively snatch His and Cys, respectively, and with no influence on the other amino acids. In addition, the largest decrease of fluorescence intensity was obtained with the input mode of Cys and His (**K**), indicating that both amino acids contributed to the decreased fluorescence (output **1**). Whichever factor quenches the fluorescence emission, output **1** is observed for the "OR" gate. Based on the integrated logic gate, the selective determination of His/Cys has been established.

Analytical performance

Under the optimal conditions, the His/Cys concentration-dependent fluorescence change was quantitatively investigated using the fluorescent CuNCs as the sensing probe. As shown in Fig. 5a, the fluorescence intensity ratio $[(I_0\text{-}I)/I_0]$ increased linearly with the concentration of His in the range of 0.05–40 μM with the addition of 100 μM NEM. The equation of the best-fit line was $(I_0\text{-}I)/I_0 = 0.033 + 0.022$ [His] ($R^2 = 0.996$), where I_0 and I are the corresponding fluorescence intensities in the absence and presence of His. The detection limit of His was estimated to be 1.6 nM at a signal-to-noise ratio of 3. As shown in Fig. 5b, a continuous increase in the fluorescence ratio $[(I_0\text{-}I)/I_0]$ was observed with the gradual addition of Cys (0.01–10 μM) in the presence of 100 μM Ni^{2+}. The equation of the best-fit line was $(I_0\text{-}I)/I_0 = 0.010 + 0.051$ [Cys] ($R^2 = 0.998$), and the detection limit of Cys was

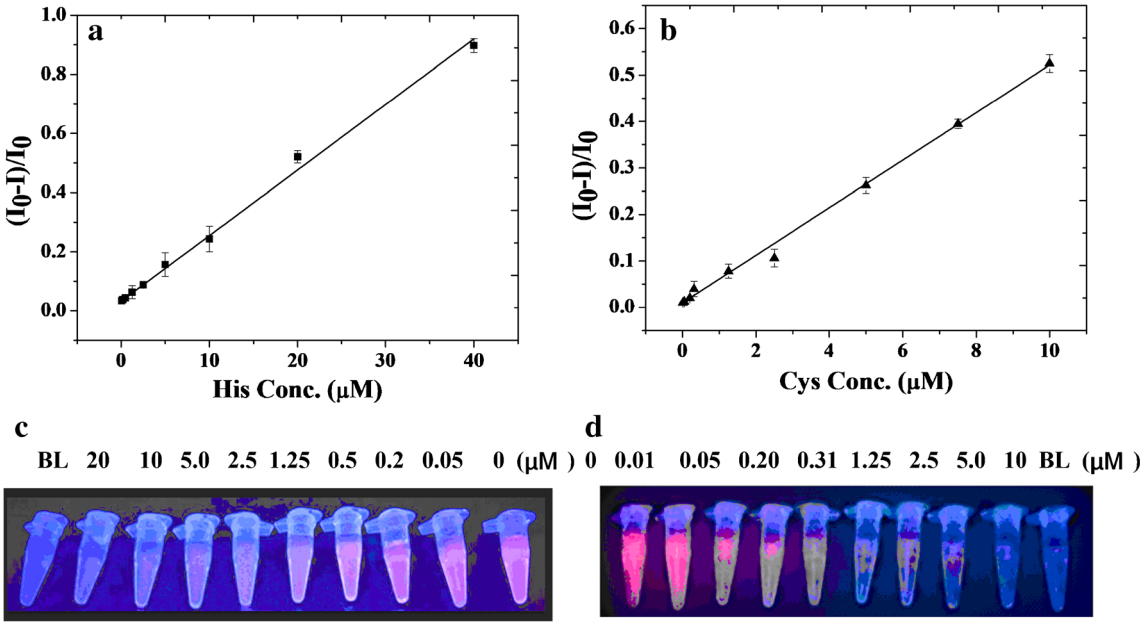

Fig. 5 Plot of FL intensity ratio $[(I_0\text{-}I)/I_0]$ versus the concentration of His (**a**) and Cys (**b**). **c** UV image for the detection of His with concentrations 0, 0.05, 0.2, 1.25, 2.5, 5.0, 10, and 20 μM; **d** UV image for the detection of Cys with concentrations 0, 0.01, 0.05, 0.20, 0.31, 1.25, 2.5, 5.0, and 10 μM. BL (blank) was the MOP solution. Measurements were performed by using 0.375 μM Loop 3, 50 μM $CuSO_4$, and 0.75 mM ascorbic acid in MOP buffer. For His detection (**a**, **c**), 10 μM Cys and 100 μM NEM were added; for Cys detection (**b**, **d**), 10 μM His and 100 μM Ni^{2+} were added. The error bars demonstrate the standard deviation for three independent measurements

estimated to be 98 pM. In addition, tolerance experiments showed that the selective detection of Cys and His was affected only slightly by the other amino acids within the concentration of 40 μM. The selectivity is comparable and even better than those of most previously reported works (Table 2). Furthermore, visual detection was possible with detection limits of 50 nM for His and 50 nM for Cys under UV radiation, which could be easily adapted to automated high-throughput screening (Fig. 5c, d).

Sample determination

In order to evaluate the practical utility of this strategy, we studied the application of the established DNA-templated

Table 2 Comparison of sensitivity in different histidine or cysteine assays

Analytical method	Analyte	Signal reporter	Detection limit
Fluorescent assay	Cys	Carbon quantum dots	2.6 nM [13]
Electrochemiluminescence	Cys	Silver nanoclusters	0.5 μM [14]
Colorimetric assay	His	Murexide	0.4 μM [19]
Fluorescent assay	His	Silver nanoclusters	1.4 μM [41]
Fluorescent assay	His	3-Azidocoumarin	76 nM [42]
Fluorescent assay	His/Cys	Thiazole orange	10/5.1 nM [28]
Fluorescent assay	His/Cys	NMM/G-4 complex	3/5 nM [29]
Fluorescent assay	His/Cys	Ag/Au bimetallic nanoclusters	87/111 nM [30]
Colorimetric assay	His/Cys	G-quadruplex-Cu(II) metalloenzyme	10/5 nM [31]
Time-resolved fluorescent assay	His/Cys	Terbium (III) coordination polymer	1.2/1 μM [32]
Fluorescent assay	Cys	Silver nanoclusters	2.1 nM for Cys [43]
Fluorescent assay[a]	His/Cys	Fluorescent CuNCs	1.6 nM/98 pM
Naked eye with UV[a]			50/50 nM

[a] This work

Table 3 Analysis of His and Cys in urine samples

Sample	Spiked (μM)		Measured (μM)		Recovery (%)		RSD (%)		Concentration in urine (μM)	
	His	Cys	His	Cys	His	Cys	His	Cys	His	Cys
1			0.296				0.13		296.0	
2	2.000		2.137		92.05		0.76			
3	5.000		5.369		101.5		0.64			
4				0.012				0.04		12.0
5		2.000		1.854		92.10		0.10		
6		5.000		5.029		100.3		0.64		
7			0.339	0.013			0.09	0.06	339.0	13.0
8	2.000	2.000	2.130	1.940	89.55	96.35	0.41	0.50		
9	5.000	5.000	5.103	5.002	95.28	99.78	0.27	0.34		

CuNC system for the direct determination of His and Cys in diluted and spiked urine samples. For the detection of His, the biological samples were treated with NEM and diluted in MOP buffer. For Cys, the samples were treated with Ni^{2+} and diluted in MOP buffer without further preparation. As shown in Table 3, the quantitative recoveries (89.55 to 101.5%) of spiked His or Cys unambiguously demonstrated that the DNA-templated CuNC system retained the sensing ability for His/Cys. There was no obvious matrix effect from the urine samples on the sensing system after the 1000-fold dilution of biological samples. These results demonstrated that the proposed method was successfully employed to detect His and Cys selectively in urine samples (Table 3).

Conclusions

In conclusion, we have developed a label and enzyme-free approach for the selective detection of histidine and cysteine by using fluorescent CuNCs as the probe. The novel protocol demonstrated several advantages. First, dumbbell DNA-templated CuNCs serves as a very good probe with highly strong fluorescence emission. Second, CuNCs are formed within several minutes in the environment-friendly condition. And the design of this approach is simple and the total sensing can be complete within about 30 min. In addition, the semi-quantitative detection of His/Cys can be observed with the naked eye under a hand-held UV lamp, which can be easily adapted to automated high-throughput screening. Third, this new system provides low detection limits of 1.6 nM for His and 98 pM for Cys, which are comparable or even better than those of most previous reports. With UV radiation, the detection limit was demonstrated to be 50 nM for each amino acid. Fourth, the assay also achieved excellent selectivity, with no interference from other natural amino acids and successful differentiation of His and Cys. Finally, the CuNC-based method is performed in homogeneous solution without any complicated separation processes, expensive equipment, and reagents. Furthermore, we are also trying to utilize the dumbbell DNA-hosted CuNCs and the target-modulated assembly reaction to further broaden its applications. Overall, our rapid assay allows for the sensitive and selective detection of Cys and His in human urine samples with no need for complicated sample pretreatment procedures.

Funding information The study was financially supported by the National Natural Science Foundation of China (No. 21505023).

Compliance with ethical standards

Conflict of interest The authors declare that they have no competing interests.

Human participation and rights This study was approved by the Institutional Review Board at Fudan University, and the experiments were performed in accordance with the ethical standards.

Informed consent The authors declare that urine samples were collected at the Fudan University and obtained with informed consent.

References

1. Mirzaei H, Suarez JA, Longo VD. Protein and amino acid restriction, aging and disease: from yeast to humans. Trends Endocrinol Metab. 2014;25:558–66.
2. Zhang SY, Ong CN, Shen HM. Critical roles of intracellular thiols and calcium in parthenolide-induced apoptosis in human colorectal cancer cells. Cancer Lett. 2004;208:143–53.
3. Shahrokhian S. Lead phthalocyanine as a selective carrier for preparation of a cysteine-selective electrode. Anal Chem. 2001;73:5972–8.
4. Gazit V, Ben-Abraham R, Coleman R, Weizman A, Katz Y. Cysteine-induced hypoglycemic brain damage: an alternative mechanism to excitotoxicity. Amino Acids. 2004;26:163–8.
5. Watanabe M, Suliman ME, Qureshi AR, Garcia-Lopez E, Bárány P, Heimbürger O, et al. Consequences of low plasma histidine in chronic kidney disease patients: associations with inflammation, oxidative stress, and mortality. Am J Clin Nutr. 2008;87:1860–6.

6. Leebeek FWG, Kluft C, Knot EAR, Demaat MPM. Histidine-rich glycoprotein is elevated in mild liver-cirrhosis and decreased in moderate and severe liver-cirrhosis. J Lab Clin Med. 1989;113:493–7.
7. Chen GN, Wu XP, Duan JP, Chen HQ. A study on electrochemistry of histidine and its metabolites based on the diazo coupling reaction. Talanta. 1999;49:319–30.
8. Li BX, Zhang ZJ, Liu ML, Xu CL. Flow injection chemiluminescence determination of L-cysteine in amino acid mixture and human urine with the BrO(3)(-)-quinine system. Anal Bioanal Chem. 2003;377:1212–6.
9. Gao C, Fan S. Influence of zone stacking sequences on CL intensity and determination of histidine in sequential injection analysis. Anal Lett. 2008;41:1335–47.
10. Wu J, Xu K, Landers JP, Weber SG. An in situ measurement of extracellular cysteamine, homocysteine, and cysteine concentrations in organotypic hippocampal slice cultures by integration of electroosmotic sampling and microfluidic analysis. Anal Chem. 2013;85:3095–103.
11. Xiao Q, Gao H, Yuan Q, Lu C, Lin JM. High-performance liquid chromatography assay of cysteine and homocysteine using fluorosurfactant-functionalized gold nanoparticles as postcolumn resonance light scattering reagents. J Chromatogr A. 2013;1274:145–50.
12. Barbaro E, Zangrando R, Vecchiato M, Turetta C, Barbante C, Gambaro A. D- and L-amino acids in Antarctic lakes: assessment of a very sensitive HPLC-MS method. Anal Bioanal Chem. 2014;406:5259–70.
13. Possari R, Carvalhal RF, Mendes RK, Kubota LT. Electrochemical detection of cysteine in a flow system based on reductive desorption of thiols from gold. Anal Chim Acta. 2006;575:172–9.
14. Feng L, Wu L, Xing F, Hu L, Ren J, Qu X. Novel electrochemiluminescence of silver nanoclusters fabricated on triplex DNA scaffolds for label-free detection of biothiols. Biosens Bioelectron. 2017;98:378–85.
15. Chen ZG, Liu JB, Han YL, Zhu L. A novel histidine assay using tetraphenylporphyrin manganese (III) chloride as a molecular recognition probe by resonance light scattering technique. Anal Chim Acta. 2006;570:109–15.
16. Hu Y, Wang Q, Zheng C, Wu L, Hou X, Lv Y. Recyclable decoration of amine-functionalized magnetic nanoparticles with Ni^{2+} for determination of histidine by photochemical vapor generation atomic spectrometry. Anal Chem. 2014;86:842–8.
17. Zhang Y, Yang RH, Liu F, Li KA. Fluorescent sensor for imidazole derivatives based on monomer-dimer equilibrium of a zinc porphyrin complex in a polymeric film. Anal Chem. 2004;76:7336–45.
18. Shao N, Jin JY, Cheung SM, Yang RH, Chan WH, Mo T. A spiropyran-based ensemble for visual recognition and quantification of cysteine and homocysteine at physiological levels. Angew Chem Int Ed. 2006;45:4944–8.
19. Sun SK, Tu KX, Yan XP. An indicator-displacement assay for naked-eye detection and quantification of histidine in human urine. Analyst. 2012;137:2124–8.
20. Chen S, Tian J, Jiang Y, Zhao Y, Zhang J, Zhao S. A one-step selective fluorescence turn-on detection of cysteine and homocysteine based on a facile CdTe/CdS quantum dots-phenanthroline system. Anal Chim Acta. 2013;787:181–8.
21. Liu YR, Hu R, Liu T, Zhang XB, Tan W, Shen GL, et al. Label-free dsDNA-Cu NPs-based fluorescent probe for highly sensitive detection of L-histidine. Talanta. 2013;107:402–7.
22. Shi F, Liu S, Su X. Dopamine functionalized-CdTe quantum dots as fluorescence probes for L-histidine detection in biological fluids. Talanta. 2014;125:221–6.
23. Bian W, Wang F, Wei Y, Wang L, Liu Q, Dong W, et al. Doped zinc sulfide quantum dots based phosphorescence turn-off/on probe for detecting histidine in biological fluid. Anal Chim Acta. 2015;856:82–9.
24. Chen X, Gong F, Cao Z, Zou W, Gu T. Highly cysteine-selective fluorescent nanoprobes based on ultrabright and directly synthesized carbon quantum dots. Anal Bioanal Chem. https://doi.org/10.1007/s00216-018-0980-3.
25. Zhang Y, Jiang J, Li M, Gao P, Zhou Y, Zhang G, et al. Colorimetric sensor for cysteine in human urine based on novel gold nanoparticles. Talanta. 2016;161:520–7.
26. Yu Y, Yang J, Xu X, Jiang Y, Wang B. A novel fluorescent probe for highly sensitive and selective detection of cysteine and its application in cell imaging. Sensors Actuators B Chem. 2017;251:902–8.
27. Miao Q, Li Q, Yuan Q, Li L, Hai Z, Liu S, et al. Discriminative fluorescence sensing of biothiols in vitro and in living cells. Anal Chem. 2015;87:3460–6.
28. Pu F, Huang Z, Ren J, Qu X. DNA/ligand/ion-based ensemble for fluorescence turn on detection of cysteine and histidine with tunable dynamic range. Anal Chem. 2010;82:8211–6.
29. Li H, Liu J, Fang Y, Qin Y, Xu S, Liu Y, et al. G-quadruplex-based ultrasensitive and selective detection of histidine and cysteine. Biosens Bioelectron. 2013;41:563–8.
30. Sun J, Yang F, Zhao D, Chen CX, Yang XR. Integrated logic gate for fluorescence turn-on detection of histidine and cysteine based on Ag/Au bimetallic nanoclusters-Cu^{2+} ensemble. ACS Appl Mater Interfaces. 2015;7:6860–6.
31. Wu C, Fan D, Zhou C, Liu Y, Wang E. Colorimetric strategy for highly sensitive and selective simultaneous detection of histidine and cysteine based on G-quadruplex-Cu(II) metalloenzyme. Anal Chem. 2016;88:2899–903.
32. Xue SF, Lu LF, Wang QX, Zhang S, Zhang M, Shi G. An integrated logic system for time-resolved fluorescent "turn-on" detection of cysteine and histidine base on terbium (III) coordination polymer-copper (II) ensemble. Talanta. 2016;158:208–13.
33. Jadzinsky PD, Calero G, Ackerson CJ, Bushnell DA, Kornberg RD. Structure of a thiol monolayer-protected gold nanoparticle at 1.1 angstrom resolution. Science. 2007;318:430–3.
34. Tao Y, Li M, Ren J, Qu X. Metal nanoclusters: novel probes for diagnostic and therapeutic applications. Chem Soc Rev. 2015;44:8636–63.
35. Liu J. DNA-stabilized, fluorescent, metal nanoclusters for biosensor development. Trac-Trends Anal Chem. 2014;58:99–111.
36. Rotaru A, Dutta S, Jentzsch E, Gothelf K, Mokhir A. Selective dsDNA-templated formation of copper nanoparticles in solution. Angew Chem Int Ed. 2010;49:5665–7.
37. Qing Z, He X, He D, Wang K, Xu F, Qing T, et al. Poly (thymine)-templated selective formation of fluorescent copper nanoparticles. Angew Chem Int Ed. 2013;52:9719–22.
38. Wang Y, Cui H, Cao Z, Lau C, Lu J. Additive and enhanced fluorescence effects of hairpin DNA template-based copper nanoparticles and their application for the detection of NAD(+). Talanta. 2016;154:574–80.
39. Wang B, Gao Y, Li HW, Hu ZP, Wu Y. The switch-on luminescence sensing of histidine-rich proteins in solution: a further application of a Cu^{2+} ligand. Org Biomol Chem. 2011;9:4032–4.
40. Liu S, Shi F, Chen L, Su X. Tyrosine-functionalized $CuInS_2$ quantum dots as a fluorescence probe for the determination of biothiols. Analyst. 2013;138:5819–25.
41. Zhou Y, Zhou TS, Zhang M, Shi GY. A DNA-scaffolded silver nanocluster/Cu^{2+} ensemble as a turn-on fluorescent probe for histidine. Analyst. 2014;139:3122–6.
42. Qiu SY, Miao M, Wang TX, Lin ZY, Guo LH, Qiu B, et al. A fluorescent probe for detection of histidine in cellular homogenate and ovalbumin based on the strategy of click chemistry. Biosens Bioelectron. 2013;42:332–6.
43. Huang ZZ, Pu F, Lin YH, Ren JS, Qu XG. Modulating DNA-templated silver nanoclusters for fluorescence turn-on detection of thiol compounds. Chem Commun. 2011;47:3487–9.